OCEANOGRAPHY

On dispersion properties of surface motions in the Gulf of Finland

Tarmo Soomere[*], Mikk Viidebaum, and Jaan Kalda

Institute of Cybernetics at Tallinn University of Technology, Akadeemia tee 21, 12618 Tallinn, Estonia

Abstract. The spreading rate of initially closely located water particles and passive drifters in the surface layer of the Gulf of Finland is studied using autonomous surface drifters. The average spreading rate increases with the increase in the time elapsed from the deployment, equivalently, with the increase in the distance between drifters. The typical spreading rate is about 200 m/day for separations below 0.5 km, 500 m/day for separations below 1 km and in the range of 0.5–3 km/day for separations in the range of 1–4 km. The spreading rate does not follow the Richardson law. The initial spreading, up to a distance of about 150 m, is governed by the power law $d \sim t^{0.27}$ whereas for larger separations the distance increases as $d \sim t^{2.5}$.

Key words: sub-grid turbulence, turbulent spreading, drifter pairs, circulation modelling, Gulf of Finland, Baltic Sea.

1. INTRODUCTION

The drift of various substances in marine environment is affected by a variety of motions, from basinwide circulation down to local processes. It is virtually impossible to exactly describe the impact of all these processes within a single modelling environment. The state-of-the-art three-dimensional (3D) circulation models adequately replicate the major features of the hydrophysical fields of natural water bodies [1] and resolve the large- and mesoscale dynamics of currents [2]. The reproduction of the details of both hydrography and patterns of currents is limited by the resolution of the model in time and space. This limitation usually does not significantly affect statistical properties of the basic hydrographical fields such as temperature, salinity or density (that are normally smoothed by local turbulence) but may substantially modify statistical properties of the drift of various substances. The reason is that even small errors in the estimates of current patterns and/or shifts in the position of the water particles due to the impact of a multitude of relatively small-scale motions (frequently called sub-grid turbulence, because it is not explicitly accounted for in the model) can drastically change the calculated

trajectories of the drift of floating objects [3,4] even when the large-scale features of trajectories are correctly captured by the underlying simulation model. The standard way to circumvent this difficulty in estimates of the current-induced drift and transport is to use ensembles of models for trajectory simulations [4] or to rely on the statistical analysis of large pools of simulations of the drift and transport patterns in sea areas with complicated dynamics [5,6].

This approach, however, still needs accounting for the processes in the sea that generally tend to separate initially closely positioned drifters. This process of gradual separation is usually attributed to the (local) turbulent spreading. The models used for studies of the Lagrangian transport should have a tool to simulate this process, otherwise the modelled particles (virtual drifters [5]) released in a single grid cell will drift together for a long time, which is usually not the case in the ocean. In other words, a successful application of any of the above methods requires a parameterization of (the impact of) the subgrid-scale processes that adequately represents the statistics of the spreading of initially close water particles at scales below the computational grid scale. When the distance between particles reaches the size of a computational grid cell, their further spreading is usually assumed to be adequately governed by the simulated velocity field.

---

[*] Corresponding author, soomere@cs.ioc.ee

The correct parameterization of subgrid-scale processes is a challenge in water bodies such as the Gulf of Finland that have very small baroclinic Rossby radius (usually 2–4 km [7]) and that host extremely complicated internal structure of motions [8,9], in particular, a large component of local rotation in the fields of currents [10]. The description of the effect of such processes requires not only following the local variations in the current speed but also accounting for the mostly circularly polarised (rotational) character of motions [11]. Moreover, in such relatively shallow water bodies it is beforehand not clear whether the spreading is governed by 3D or quasi-two-dimensional (2D) constituents of the turbulence.

The primary measure of spreading is the rate of increase in the distance of initially closely located water particles (equivalently, passive drifters). This rate is not constant and can be approximated by a power function or an exponential law of the time elapsed from the release of the particles [12]. This paper describes an attempt to experimentally quantify this rate in the surface layer owing to small-scale turbulence in the Gulf of Finland using partially submerged lightweight autonomous floating buoys. Differently from a number of similar earlier studies [13–16], we concentrate on relatively small initial distances of the drifters (about 100 m). We start from an overview of the expected properties of turbulent spreading in natural water bodies followed by the description of the devices and the raw data. The statistical analysis of trajectories of initially closely located drifters is performed next to quantify the dependence of the spreading rate on the elapsed time and on the instantaneous distance between the drifters. The analysis reveals that the underlying dynamics apparently is a mixed regime of 2D and 3D motions.

2. THEORETICAL SPREADING RATES

The law describing the evolution of the average distance between two particles (the drifters, in our case), which are being transported by a turbulent velocity field, is most often referred to as the Richardson law [12]. This concept applies in the case of classical example of fully developed 3D turbulent flows where the average (scalar) difference between velocity fluctuations $\mathbf{v}(\mathbf{r}, t)$ follows the (Kolmogorov) power law $\langle |\mathbf{v}(\mathbf{r}, t) - (\mathbf{r} + \Delta\mathbf{r}, t)| \rangle = A |\Delta\mathbf{r}|^a$ [17]. Here angle brackets denote averaging over the coordinate $\mathbf{r}$ and/or over the ensemble of flows, A is a constant and the exponent $a = 1/3$ is specific to the fully developed 3D turbulent flow.

The Richardson pair dispersion law states that, optionally after a short section of so-called ballistic dispersion (when the average distance d between a pair of tracers increases linearly with time [15]) in such flows scales as $d \propto t^b$, where $b = 1/(1 - a)$. This law can be, heuristically, easily derived by noting that the growth rate in the distance d is dominated by the action of the largest vortex, separating the two particles. The size of such a vortex is approximately the distance d. Therefore, the rotation (stretching) time is estimated as $t \approx d/(Ad^a)$ and, hence, the distance d increases roughly proportionally to the power law $d \propto t^{1/(1-a)}$. In the case of the Kolmogorov law $a = 1/3$ and the corresponding exponent is $b = 3/2$. The relative dispersion D^2 and the relevant diffusivity coefficient can be obtained from the distance d as an average value $D^2(t) = \langle d^2(t) \rangle$ over all pairs [15].

In many cases the system of large-scale motions in the ocean and in the atmosphere is almost two-dimensional. The situation with spreading is essentially different in 2D flows where at scales smaller than the energy input scale, the velocity spectrum is dominated by the enstrophy cascade and $a = 1$. The exponent b in the Richardson law, formally, turns to infinity in this case and an exponential growth of the distance with time (the Lin law) occurs [16–18]. Thus, for an ideal 2D turbulence with a single energy input scale λ, while the Lin law is expected to be valid for scales below λ, Richardson law is related to large-scale circulation [19]. Both these flow regimes have been observed in the open ocean [13] and in the Baltic Sea for different scales [14]. Contrary to the above-mentioned theoretical expectation, it has been reported that the Richardson law fairly well describes spreading properties for small distances whereas the Lin law shows a better fit for large distances [14].

The situation is more complicated for transport by 2D surface flows occurring on the surface of 3D flows. Such flows are generally partly compressible. The compressibility is defined as the relative weight of the potential component in the decomposition of the net velocity field into solenoidal and potential components. At the free-slip surface of a 3D turbulent incompressible fluid, the compressibility of the 2D velocity field is approximately 0.5. The presence of compressibility can result in a considerable decrease in the pair dispersion exponent b [20,21] (for a review of relevant laboratory experiments see [22]). On the other hand, if the water flow is intrinsically 2D, the surface flow follows the bulk flow, resulting in zero compressibility. As many geophysical flows are mixtures of 2D and 3D flows, for such flows in the oceans and the atmosphere one might expect quite a large variation in the exponent b; it may take a value in the range from 1.5 to infinity, depending on the particular flow situation. In this paper we make an attempt to estimate the resulting finite value of the exponent b in the conditions of the Gulf of Finland and leave the question of the role of different physical effects shaping its value to further studies.

3. EXPERIMENTS

The experiments were performed in the western and central part of the Gulf of Finland (Fig. 1). This gulf is an elongated relatively shallow water body in the north-eastern Baltic Sea with a length of over 400 km, a mean depth of 37 m and the width varying from 48 to 135 km [23]. The dynamics of water masses in its western part is strongly affected by the impact of the open part of the Baltic Sea: a continuous water exchange occurs between the two water bodies without a sill in between [8,24]. Its eastern end receives the largest single fresh water inflow to the Baltic Sea (the Neva River) and buoyancy-driven currents thus play an important role in the circulation in this basin [23,25]. The result is a strong east-west gradient in salinity and sea level, extremely complicated horizontal and vertical structure and temporal variation of salinity, and high variability in temperature and velocity fields that also undergo substantial seasonal variations owing to a similar course in the wind field and the incoming solar radiation [2,8,26]. The system of currents in the Gulf of Finland reveals a complicated pattern of basin-scale mostly cyclonic circulation, optionally anticyclonic gyre in the surface layer in the eastern part of the gulf [6], exchange of water masses with the Baltic Proper, a variety of mesoscale synoptic eddies and frequent 3D effects such as upwelling [8,25–27].

The success of the modelling efforts in this basin strongly depends on the used horizontal and vertical resolution. In order to properly resolve mesoscale dynamics, it is necessary to use the horizontal grid size not larger than about ½ of the Rossby radius [28]. Therefore, the circulation models for the Gulf of Finland with a spatial resolution of about 2 nautical miles (3.7 km) [2,6] are barely eddy-permitting and only conditionally reproduce the basic patterns of motions, whereas for an adequate reproduction of mesoscale current patterns the grid step should be ≤2 km [29,30]. The models with a resolution coarser than 3.7 km are superseded by now. Therefore, it is reasonable to assume that at scales larger than about 4–5 km the spreading and transport properties are reasonably resolved by the majority of the models of the Gulf of Finland. For this reason, we concentrate on spreading properties of small-scale features up to distances of a few kilometres between the drifters.

The spreading of passive drifters in the surface layer of the Gulf of Finland is studied experimentally using prototypes of lightweight autonomous floating buoys (Fig. 2), constructed and manufactured by the PTR Group (Tallinn, Estonia) based on the solution from the Wave Engineering Laboratory, Institute of Cybernetics. The active component (CT-24, Sanav Corp., Taiwan) is a high sensitivity (–159 dB) GPS/GSM device, which in our case connects to the 1800 MHz GSM network. The device was set to report its position 4 times an hour as a standard SMS message (NMEA 0183 GPRMC sentence) over the TCP protocol to a FTP server. The active device was mounted on the top of a 2 m long and 50 mm in diameter plastic pipe. The capacity of eight D-size standard elements (18 Ah) together with the internal Li-ion battery (3.7 V, 18 Ah) enabled continuous work of the device for 2–3 weeks. The batteries and deadweight were mounted at the other end of the pipe to adjust the buoyancy of the device. The working position of the drifters was vertical: about 2/3 of the pipe was submerged and about 1/3 (60 cm) above the water surface. This construction made it possible to transmit GSM signal to coastal stations from a distance up to 30 km offshore.

Three deployments were made with altogether 8 drifters and with drifting time from a few days to several weeks in August–October 2010 (Table 1). In each experiment, three drifters were deployed at a distance of about 50–150 m from each other. Two

Fig. 1. Location scheme of the Baltic Sea and the Gulf of Finland.

Fig. 2. A view of the drifter and a block of eight standard D-size batteries. This figure is available in colour at http:/www.eap.ee.

Table 1. Parameters of drifter experiments

Date of deployment	Deployment locations	No. of the deployed drifters in Figs 4, 5	Pairs in Fig. 7	Drifter time on sea, days
15.06.2010	3 different locations around Naissaar 59°31′50″N; 24°21′8″E	Testing		–
12.08.2010	8 km west of Naissaar 59°32′50″N; 24°21′3″E	T4, T5, T6	T4, T5 = Pair 1 T5, T6 = Pair 2 T4, T6 = Pair 3	11–25
26.08.2010	8 km west of Naissaar 59°32′22″N; 24°22′1″E	T7, T8	Pair 4	9–15
22.09.2010	Muuga Bay 59°34′12″N; 24°55′24″E	T9, T10, T11	T9, T10 = Pair 5 T10, T11 = Pair 6 T9, T11 = Pair 7	3–13

deployments took place about 8 km west of the Island of Naissaar and one in Muuga Bay. The deployments resulted in 7 pairs of drifter trajectories that allowed calculation of the temporal evolution of the separation of the counterparts.

During the first deployment week 12.–19.08 the weather was stable and calm. The winds blew dominantly from the south and south-east but the direction largely varied during the week. The hourly average wind speed was mostly in the range of 3–5 m/s (the weekly average 2.8 m/s) and only on 19.08 reached values close to 8 m/s. The conditions on the sea were almost the same during the week. The weather was even calmer during the first part of the week (26.08–02.09) after the second deployment. Wind speed slightly increased (to the level of about 7 m/s, single gusts up to 19 m/s) on 2–3 September. The third deployment was performed under slightly higher southerly and south-easterly winds at the end of September (Fig. 3). On 27.–29.09 the wind speed was about 8 m/s for almost two days and reached values close to 10 m/s on 28.09. Although such wind speeds are quite moderate, they are able to excite waves with significant wave height of about 1 m. The presence of relatively high waves is the most probable reason why the signal from one of the drifters was lost for ten days (during which the buoy drifted some 80 km to the west).

The observed trajectories reflect a variety of pheno-mena, characteristic to the current field of the Gulf of Finland (Figs 4, 5): the presence of relatively small mesoscale eddies with a diameter of about 5 km to the north of Naissaar, inertial oscillations in the open part of the gulf to the north of Pakri Peninsula and further north of Naissaar, and relatively rapid almost straight alongshore drift apparently steered by topography. While most of the trajectories are relatively short (below 50 km), one alongshore drifting device covered more than 150 km during about two weeks and left the Gulf of Finland to the Baltic Proper (Fig. 5).

Let us estimate the contribution of the wind to the overall drift velocity. Assuming that both air and water friction are dominated by turbulent drag, the net force due to air is $\frac{1}{2}k_a A_a \rho_a v_a^2$ and that due to water $\frac{1}{2}k_w A_w \rho_w v_w^2$. Here v_i stands for the relative velocity of the buoy with respect to the water ($i = w$) or air ($i = a$), A_i denotes the surface area subject to the water of air drag, k_i is the ratio of the cross-section areas of the turbulent tail and the buoy, and ρ_i are the densities of water and air. In the stationary case, the two forces compensate each other, so that $\frac{1}{2}k_a A_a \rho_a v_a^2 = \frac{1}{2}k_w A_w \rho_w v_w^2$.

Using here $2A_a = A_w$ (corresponding to the under-water and above-water lengths of the buoy), $820\rho_a = \rho_w$, and assuming that $k_a = k_w$, we end up with the following estimate of the speed for wind-induced drift of the device: $v_w \approx 0.025 v_a$. For the wind speed of $v_a = 5$ m/s, this yields a contribution to the drift speed of $v_w \approx 12$ cm/s. Although this value is of the order of the current speed, its contribution to the increase in the distance between the drifters apparently is much lower. Namely, this increase appears not because of the average drag by water and air (which affects all the buoys in the same way) but because of turbulent pulsations of these flows. Moreover, low winds over almost calm sea surface are relatively smooth (much more laminar) compared to similar winds over the mainland, due to the absence of major obstacles above the sea surface. Therefore, it is natural to expect that the impact of wind on the clusters and pairs of closely located drifters becomes mostly evident as their concurrent downwind drift.
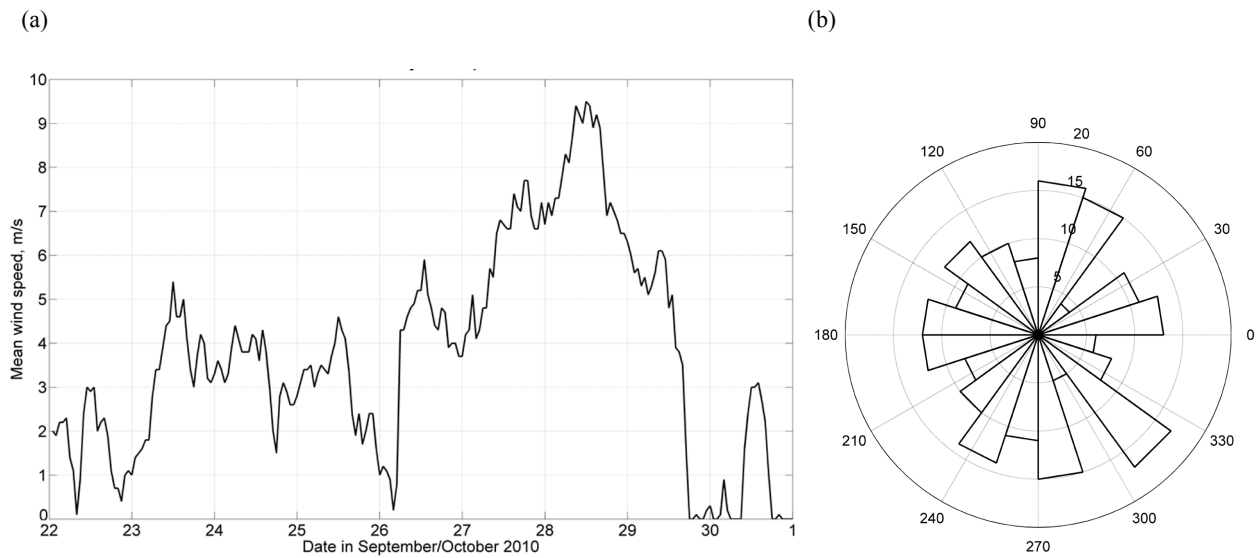
(a)

(b)

Fig. 3. Hourly mean wind speed (a) and wind rose (b) for the first week of the third deployment.
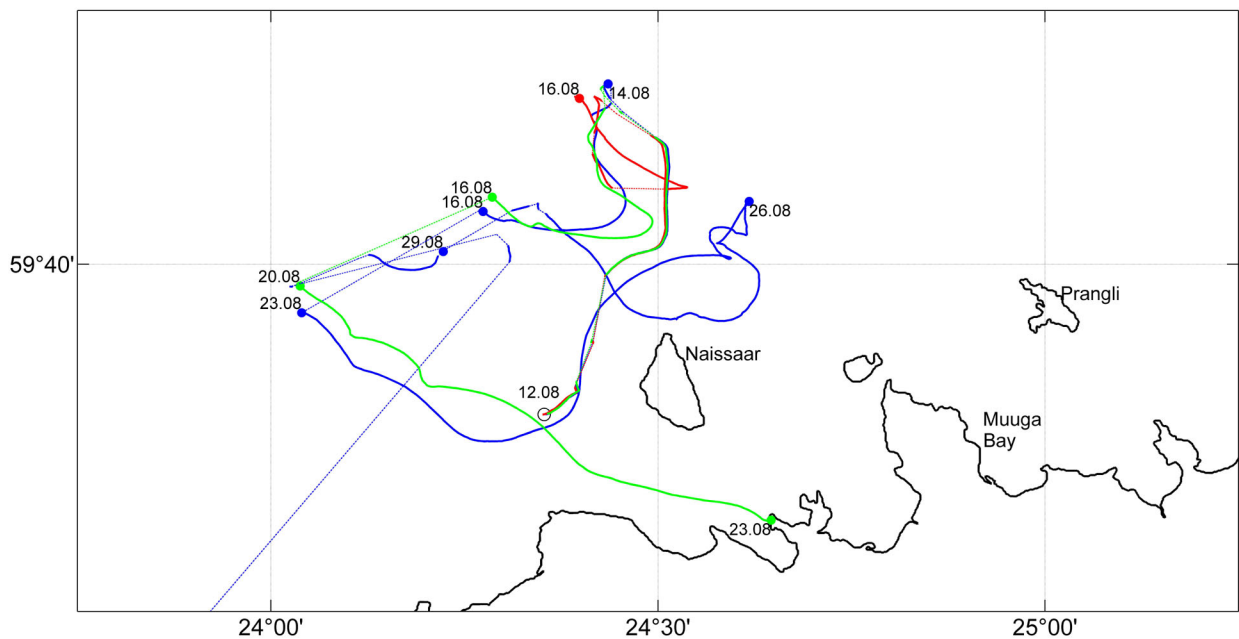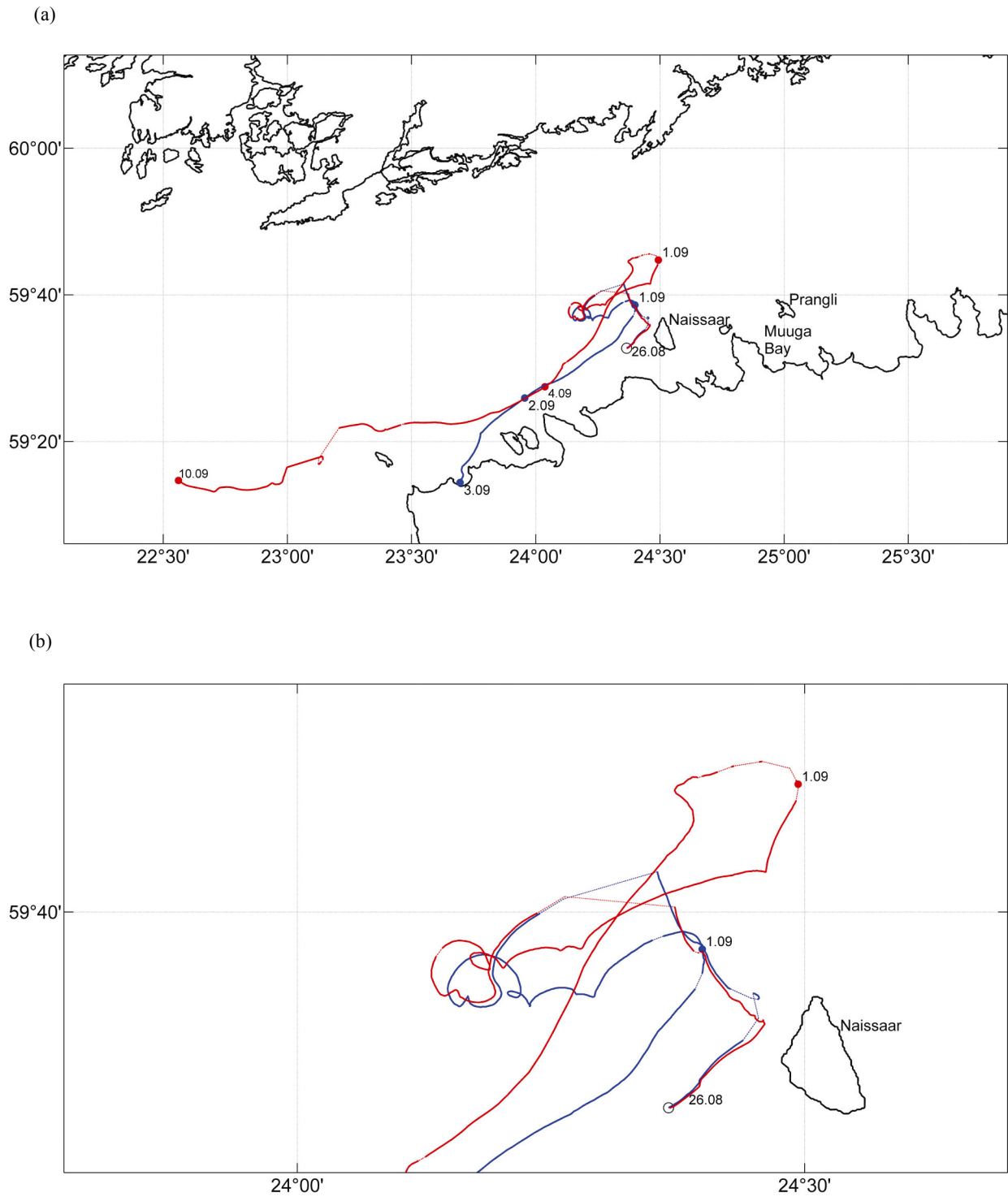

Fig. 4. Trajectories of drifters deployed on 12.08.2010 (black – T4, gray – T5, light gray – T6) in open sea to the west of Naissaar. The deployment site is indicated by the empty circle. Thin straight sections of the trajectories represent intervals when the GSM signal (and the details of the trajectories) was not available. This figure is available in colour at http:/www.eap.ee.

(a)

(b)

Fig. 5. Trajectories of drifters deployed on 26.08.2010 (blue – T7, red – T8); (a) – the entire field of motions; (b) – trajectories in a sea area near Naissaar. Other notations are the same as for Fig. 4. This figure is available in colour at http:/www.eap.ee.

4. SPREADING RATE

Below we consider the measured distance d between drifters in pairs and the rate of increase (spreading rate) in this distance. The values for relative dispersion D^2 and the diffusivity coefficient can be obtained from the presented results in a straightforward manner [15]. As expected from the above considerations, the spreading rate depends heavily on the time elapsed from deployment and, therefore, on the instantaneous distance between the drifters (Table 2). The rate is estimated separately for each pair as the travel distance (100 m, 200 m, etc) divided by the time needed to increase the separation from 100 to 200 m, from 200 to 400 m, from 400 to 800 m, etc. For smaller initial separations we used partially overlapping ranges because of the small number of pairs with such properties. The estimates for initial distances below 100 m should be interpreted as indicative because of possible uncertainties of GPS-measured locations. The typical spreading rate of drifters initially separated by less than 1 km varied from about 100 to 700 m/day (Fig. 6). This rate was almost constant for all the pairs within the first 10–15 h of the deployment until the drifters were separated by about 150 m (see insert in Fig. 4). Such a behaviour suggests the presence of different regimes of spreading (either ballistic or Richardson's law) for initially very closely located drifters up to separations of about 150 m and for the pair with larger separations.

For even larger distances between the drifters (starting from about 600 m) the spreading rate revealed somewhat different behaviour for different pairs. The separation distance considerably (at times by a factor of two) and persistently increased for several pairs. For some other pairs the distance revealed substantial quasi-regular oscillations. This phenomenon may have been caused by the impact of relatively small mesoscale eddies with a diameter as small as about 400 m.

Table 2. Average spreading rate for different distances between the drifters

Distance between the drifters, m	Spreading rate, m/day
30–60	60
50–100	120
75–150	310
100–200	500
200–400	760
400–800	930
800–1600	3100
1600–3200	1680
3200–6400	5000

* The estimates for the separations >3 km are based on two pairs only (Fig. 6) and should be interpreted as indicative.
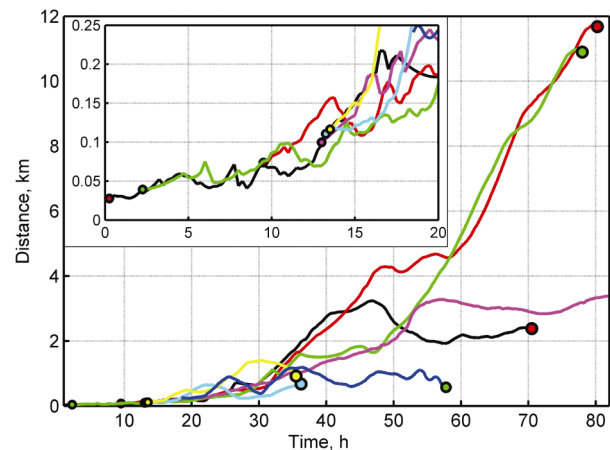
Fig. 6. Temporal course of the distance between pairs in linear coordinates. Circles show the beginning and the end of sensible measurements of the pairs' locations. The beginning time of deployments is chosen so that the initial separation of each pair matches the average distance of pairs deployed with initially smaller separation. The insert shows the pairs' separation during the first 20 h. This figure is available in colour at http:/www.eap.ee.

The presented data suggests that the structure of small-scale turbulence in the study area may contain motions of substantially different character at different scales. The substantial decrease in the average spreading rate for distances of 1.6–3.2 km (cf. Fig. 6) suggests that the dynamics may be strongly impacted by the presence of coherent structures of approximately the same size. This conjecture matches the small values of the baroclinic Rossby radius for some parts of the experiment area [7], according to which long-living eddies with a diameter of 1–2 km may frequently occur in this area.

The resulting data can be used for the design of a realistic parameterization of sub-grid-scale processes in the Gulf of Finland. The desired parameterization will strongly depend on the resolution of the ocean model, equivalently, on the particular threshold for the subgrid-scale motions. First of all, models with spatial resolution coarser than 2 km apparently cannot resolve mesoscale dynamics in this region. If, however, they are used by some reason, the parameterization of subgrid-scale processes should correspond to a typical spreading rate of about 2 km/day. The same rate of spreading can be recommended for models with a resolution of about 1–2 km while the models with a resolution of about 1 km might use the rate of about 700 m/day. Parameterizations leading to spreading rates of 300–500 m/day may be recommended for extremely high-resolution models with a grid step of about 0.5 km [11].

It is important to underline that the discussed rates apparently contain a substantial amount of impact from mesoscale eddies that, ideally, should be resolved by the hydrodynamic model. The spreading rate owing to the

impact of basically random component of turbulent fields (random walk regime [15]) can be estimated from the initial sections (the parts that reveal no extensive quasi-periodic variations due to coherent structures) of the temporal course of the drifters' distance in Fig. 4. This rate is mostly in the range of 200–300 m/day, that is, about twice as large as hypothesized in simulations in [11].

5. POWER LAW REPRESENTATION

It is interesting to analyse whether the dynamics of the study site is mostly governed by 3D (local) turbulence or by 2D (large-scale) motion system. Figure 7 presents the temporal course of the distance between drifter pairs in linear-power law coordinates, with the exponent 2/3 corresponding to the theoretical spreading rate for the 3D turbulence. The distance between the pairs of drifters increases approximately linearly in these coordinates only until values of about 400 m (equivalently, during about 25 h), after which the separation rate starts to increase for the majority of pairs. Remarkably, only two pairs (2 and 3 in Fig. 7) reveal a linear increase in the distance in this framework and thus an almost perfect match for the theoretical considerations for the 3D turbulence in a later stage of evolution. This happens after 2–2.5 days of drifting when the distance between the drifters was more than 4 km.

As the baroclinic Rossby radius for the study area is a few kilometres [23], such behaviour indicates that the drifters evidently were involved in very different motion systems. These pairs (drifters T4, T5, and T6) have been deployed on 12.08.2010 (Fig. 4, Table 1) in relatively calm weather conditions. The shape of trajectories in Fig. 4 suggests that all three drifters were involved in a
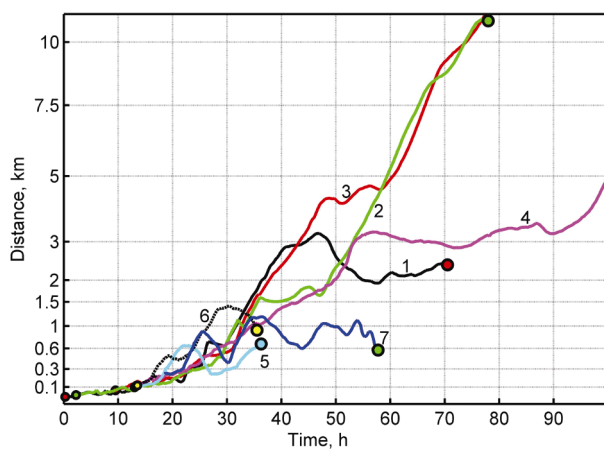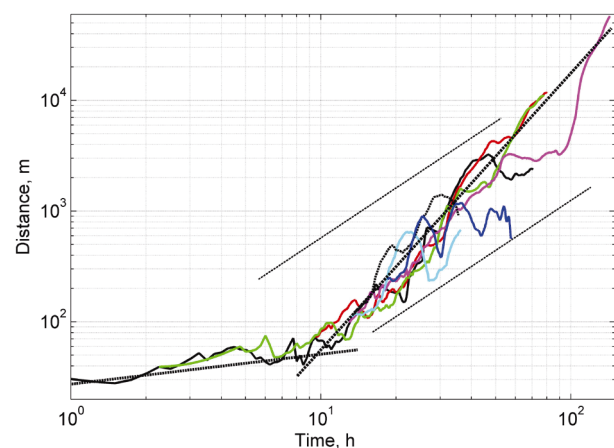
relatively large-scale system of motion that carried them almost together during the first two days on sea. The drift direction abruptly turned by 180° on 14.08, after which the drifters were carried almost exactly along their former trajectory during some time. The signal was lost on 16.08 for a few days. Although the connection was restored on 20.08, we only used the data from the first four days in the analysis.

The search for the best fit of the exponent b in the power law $d \sim t^b$ was performed using regression analysis for the dependence of the distance on the time in log-log coordinates. For relatively small separations (below 70 m in the initial phase of the drift, up to 8 h) the increase in distance is approximately linear (Fig. 8). Starting from a separation of about 100 m and a drift time of 10 h, this increase occurs much faster. The exponent b for the initial phase of the drift is in the range 0.23–0.3, with the mean value of 0.27. Such low values signify that the separation rate is governed by a ballistic law rather than by the Richardson law. Moreover, none of these laws dominates; therefore certain specific mechanisms, such as shear dispersion (particle separation due to variation of the mean velocity field) and specific surface-layer dispersion (induced by the gradient of the energy dissipation rate in the turbulent surface layer [31]) govern the particle separation rate in the study area.

Drifters in pairs 5 and 6 in Fig. 7 evidently were involved into large-scale coherent motions and their behaviour apparently was less impacted by random turbulence. This is reflected by the best fit for the exponent b for these pairs (1.3 and 0.88, respectively). All other pairs reveal surprising match of the spreading

Fig. 7. Temporal course of the distance between pairs of drifters in linear-power law 2/3 coordinates. This figure is available in colour at http:/www.eap.ee.

Fig. 8. Temporal course of the distance between pairs of drifters in log-log coordinates. Bold dashed lines correspond to the power laws with $b = 0.27$ (time interval 1–10.5 h) and $b = 2.5$ (time interval 8–105 h). Dashed lines correspond to the Richardson law with $b = 1.5$. This figure is available in colour at http:/www.eap.ee.

rates although the temporal course of their spreading is seemingly very different. The exponent b varies from 2.12 to 2.72, with the average value of about 2.5.

A fairly similar result can be obtained via regression analysis of the dependence of the average distance on the drift time. This analysis results in an estimate $b \approx 2.2$ if all the pairs are involved and, not surprisingly, $b \approx 2.5$ if the above-mentioned pairs, showing coherent motion, are excluded. Both resulting values are of a reasonable magnitude compared to the infinite exponent characterizing 2D flows but yet clearly larger then the classical Richardson value $b = 1.5$, characteristic to the 3D turbulent motions. Therefore, in the study area the dynamics is predominantly governed by 3D flows, but the contribution of a 2D motion system is still substantial.

6. DISCUSSION AND CONCLUSIONS

The presented results have a direct application in recent attempts to use the Lagrangian dynamics of the currents to develop methods for the reduction of environmental risks [6,29,30]. These attempts explore the potential for an increase in the time during which an adverse impact (for example, an oil spill) reaches a vulnerable area after an accident has happened. They use a statistical analysis of large sets of Lagrangian trajectories of virtual drifters or water particles. These trajectories (and, consequently, the probability of hitting a vulnerable area or the time it may take for the pollution to reach such areas) are highly sensitive with respect to the parameterization of subgrid-scale processes that may randomly redirect drifters to largely different sea areas compared to the modelled fields of currents [11,32–34]. The problem is even more complicated in strongly stratified sea areas such as the Gulf of Finland where the drift is frequently steered by multilayered dynamics [9] and it is not clear beforehand which theoretical framework (predomination of 2D or 3D motion systems) should be used in the analysis. Similar problems intrinsically arise in attempts of modelling of pathways of different water masses [34] and especially in model simulations, both in forecast and hindcast modes, of actual pollution transport by 3D hydrodynamic models such as HIROMB or Seatrack Web [35,36].

The analysis reveals that the well-known Richardson law for the increase in the distance between passive drifters does not become evident in the Gulf of Finland conditions. The initial evolution of closely located drifters to some extent resembles the ballistic law but a power law $d \sim t^{0.27}$ much better describes the spreading in the range of distances from the first tens of metres up to about 100–150 m. Starting from this threshold, the distance increases, on average, according to a power law $d \sim t^{2.5}$.

The presented results are to some extent affected by the impact of the local wind and waves on the drift of the used devices that extend by about 60 cm above water surface. Air flow at these heights is substantially modified by the presence of the water surface and the wind speed at these heights is considerably smaller than that at the standard height of measurements (10 m). In almost calm conditions (wind speed <3 m/s, during about a half of the duration of the experiments) the realistic wind-induced additional drift speed apparently is a few cm/s. In fresh wind conditions the wind speed over surface waves is additionally damped and the relevant drift apparently is also small. In rougher seas the drifters evidently feel stronger wave-induced drift. As the low wind and wave fields are relatively homogeneous in the open sea, most of the wind- and wave-induced impact apparently contributes towards synchronous drift of the pairs rather than towards their spreading. Therefore, the presented rates may to some extent overestimate the actual spreading rates but the order of magnitude for the spreading effects extracted from the experiments evidently is realistic.

The spreading rate of drifters on the sea surface, as expected, substantially depends on their instantaneous distance. This rate experiences fairly limited variations for small separations (<150 m) where it is 200–300 m/day. Starting from separations from about 200 m, the trajectories are frequently affected by coherent motions with scales about 400 m. This suggests that ocean models with an effective resolution down to 0.5 km might be necessary to properly resolve the mesoscale motions.

REFERENCES

1. Kantha, L. M. and Clayson, C. A. *Numerical Models of Oceans and Oceanic Processes*. Academic Press, San Diego, San Francisco, 2000.

2. Myrberg, K., Ryabchenko, V., Isaev, A., Vankevich, R., Andrejev, O., Bendtsen, J., Erichsen, A., Funkquist, L., Inkala, A., Neelov, I. et al. Validation of three-dimensional hydrodynamic models in the Gulf of Finland based on a statistical analysis of a six-model ensemble. *Boreal Env. Res.*, 2010, **15**, 453–479.

3. Griffa, A., Piterbarg, L. I., and Ozgokmen, T. Predictability of Lagrangian particle trajectories: effects of smoothing of the underlying Eulerian flow. *J. Mar. Res.*, 2004, **62**, 1–35.

4. Vandenbulcke, L., Beckers, J.-M., Lenartz, F., Barth, A., Poulain, P.-M., Aidonidis, M., Meyrat, J., Ardhuin, F., Tonani, M., Fratianni, C. et al. Super-ensemble techniques: Application to surface drift prediction. *Progr. Oceanogr.*, 2009, **82**, 149–167.

5. Soomere, T., Viikmäe, B., Delpeche, N., and Myrberg, K. Towards identification of areas of reduced risk in the Gulf of Finland, the Baltic Sea. *Proc. Estonian Acad. Sci.*, 2010, **59**, 156–165.

6. Soomere, T., Delpeche, N., Viikmäe, B., Quak, E., Meier, H. E. M., and Döös, K. Patterns of current-induced transport in the surface layer of the Gulf of Finland. *Boreal Env. Res.*, 2011, **16** (Suppl. A), 49–63.

7. Alenius, P., Nekrasov, A., and Myrberg, K. The baroclinic Rossby-radius in the Gulf of Finland. *Cont. Shelf Res.*, 2003, **23**, 563–573.

8. Andrejev, O., Myrberg, K., Alenius, P., and Lundberg, P. A. Mean circulation and water exchange in the Gulf of Finland – a study based on three-dimensional modelling. *Boreal Env. Res.*, 2004, **9**, 1–16.

9. Gästgifvars, M., Lauri, H., Sarkanen, A.-K., Myrberg, K., Andrejev, O., and Ambjörn, C. Modelling surface drifting of buoys during a rapidly-moving weather front in the Gulf of Finland, Baltic Sea. *Estuar. Coast. Shelf Sci.*, 2006, **70**, 567–576.

10. Lilover, M.-J., Pavelson, J., and Kõuts, T. Wind forced currents over shallow Naissaar Bank in the Gulf of Finland. *Boreal Env. Res.*, 2011, **16** (Suppl. A), 164–174.

11. Andrejev, O., Sokolov, A., Soomere, T., Värv, R., and Viikmäe, B. The use of high-resolution bathymetry for circulation modelling in the Gulf of Finland. *Estonian J. Eng.*, 2010, **16**, 187–210.

12. Richardson, L. F. Atmospheric diffusion shown on a distance-neighbour graph. *Proc. Roy. Soc. A*, 1926, **110**, 709–737.

13. Ollitrault, M., Gabillet, C., and Colin de Verdiere, A. Open ocean regimes of relative dispersion. *J. Fluid Mech.*, 2005, **533**, 381–407.

14. Döös, K. and Engqvist, A. Assessment of water exchange between a discharge region and the open sea – a comparison of different methodological concepts. *Estuar. Coast. Shelf Sci.*, 2007, **74**, 709–721.

15. Lumpkin, R. and Elipot, S. Surface drifter pair spreading in the North Atlantic. *J. Geophys. Res.*, 2010, **115**, Art. No. C12017.

16. Lin, J. T. Relative dispersion in the enstrophy-cascading inertial range of homogeneous two-dimensional turbulence. *J. Atm. Sci.*, 1972, **29**, 394–396.

17. Falkovich, G., Gawedzki, K., and Vergassola, M. Particles and fields in fluid turbulence. *Rev. Mod. Phys.*, 2001, **73**, 913–975.

18. LaCasce, J. H. Statistics from Lagrangian observations. *Progr. Oceanogr.*, 2008, **77**, 1–29.

19. Salazar, J. P. L. C. and Collins, L. R. Two-particle dispersion in isotropic turbulent flows. *Annu. Rev. Fluid Mech.*, 2009, **41**, 405–432.

20. Bec, J., Gawedzki, K., and Horvai, P. Multifractal clustering in compressible flows. *Phys. Rev. Lett.*, 2004, **92**, Art. No. 224501.

21. Kalda, J. Sticky particles in compressible flows: Aggregation and Richardson's law. *Phys. Rev. Lett.*, 2007, **98**, Art. No. 064501.

22. Cressman, J. R., Davoudi, J., Goldburg, W. I., and Schumacher, J. Eulerian and Lagrangian studies in surface flow turbulence. *New J. Phys.*, 2004, **6**, Art. No. 53.

23. Soomere, T., Myrberg, K., Leppäranta, M., and Nekrasov, A. The progress in knowledge of physical oceanography of the Gulf of Finland: a review for 1997–2007. *Oceanologia*, 2008, **50**, 287–362.

24. Elken, J., Raudsepp, U., and Lips, U. On the estuarine transport reversal in deep layers of the Gulf of Finland. *J. Sea Res.*, 2003, **49**, 267–274.

25. Alenius, P., Myrberg, K., and Nekrasov, A. Physical oceanography of the Gulf of Finland: a review. *Boreal Env. Res.*, 1998, **3**, 97–125.

26. Andrejev, O., Myrberg, K., and Lundberg, P. A. Age and renewal time of water masses in a semi-enclosed basin – application to the Gulf of Finland. *Tellus*, 2004, **56A**, 548–558.

27. Lehmann, A. and Myrberg, K. Upwelling in the Baltic Sea – a review. *J. Marine Syst.*, 2008, **74**, S3–S12.

28. Drijfhout, S. S. Eddy-genesis and the related heat transport: A parameter study. In *Mesoscale/Synoptic Coherent Structures in Geophysical Turbulence* (Nihoul, J. C. J. and Jamart, B. M., eds). Elsevier Oceanography Series, 1989, **50**, 245–263.

29. Andrejev, O., Soomere, T., Sokolov, A., and Myrberg, K. The role of spatial resolution of a three-dimensional hydrodynamic model for marine transport risk assessment. *Oceanologia*, 2011, **53**(1-TI), 309–334.

30. Soomere, T., Viikmäe, B., Delpeche, N., and Myrberg, K. Towards identification of areas of reduced risk in the Gulf of Finland, the Baltic Sea. *Proc. Estonian Acad. Sci.*, 2010, **59**, 156–165.

31. Skvortsov, A., Jamriska, M., and DuBois, T. C. Scaling laws of passive tracer dispersion in the turbulent surface layer. *Phys. Rev. E*, 2010, **82**, 5, Art. No. 056304.

32. Döös, K. Inter-ocean exchange of water masses. *J. Geophys. Res.*, 1995, **100**, C13499–C13514.

33. de Vries, P. and Döös, K. Calculating Lagrangian trajectories using time-dependent velocity fields. *J. Atm. Oceanic. Technol.*, 2001, **18**, 1092–1101.

34. Meier, H. E. M. Modeling the pathways and ages of inflowing salt- and freshwater in the Baltic Sea. *Estuar. Coast. Shelf Sci.*, 2007, **74**, 610–627.

35. Funkquist, L. HIROMB, an operational eddy-resolving model for the Baltic Sea. *Bull. Maritime Inst. Gdańsk*, 2001, **28**, 7–16.

36. Gästgifvars, M., Ambjörn, C., and Funkquist, L. Operational modelling of the trajectory and fate of spills in the Baltic Sea. In *Proc. 25th Arctic and Marine Oil-spill Program (AMOP) Technical Seminar, Calgary, Canada, 2001.* Environment Canada, 2002, 1115–1130.

Soome lahe pinnakihi hoovuste dispersioonist

Tarmo Soomere, Mikk Viidebaum ja Jaan Kalda

On analüüsitud veeosakeste dispersiooni parameetreid Soome lahe pinnakihis Naissaare ja Prangli piirkonnas tehtud eksperimentide alusel. Dispersiooni omadused määratleti lähestikku paigutatud autonoomsete ujuvpoide paaride triivi alusel. Paaride lahknemise kiirus kasvab oluliselt koos poidevahelise vahemaa suurenemisega. Teineteisest ligikaudu 500 m kaugusel paiknevate poide lahknemise tüüpiline kiirus on 200 m päevas, 1 km kaugusel paiknevate poide puhul 500 m päevas ja 1–4 km vahekaugusega poide puhul vahemikus 0,5–3 km päevas. Lahknemise analüüs näitab, et kõnesolevas piirkonnas ei avaldu Richardsoni seadus $d \sim t^{1.5}$. Kuni vahemaadeni 150 m toimub lahknemine vastavalt astmeseadusele $d \sim t^{0.27}$ ja suuremate vahemaade puhul vastavalt astmeseadusele $d \sim t^{2.5}$.